Innovative Food Science and Emerging Technologies 91 (2024) 103541

Contents lists available at ScienceDirect

Innovative Food Science and Emerging Technologies

journal homepage: www.elsevier.com/locate/ifset

The emulsifying performance of brewers' spent grains treated by colloid milling

Yi Ling Chin [a,b,c], Somayeh Taghian Dinani [a], Wei Ning Chen [b,c], Remko Boom [a,*]

[a] Laboratory of Food Process Engineering, Wageningen University, PO Box 17, 6700, AA, Wageningen, the Netherlands
[b] Food Science and Technology Programme, Nanyang Technological University, 62 Nanyang Drive, 637459, Singapore
[c] School of Chemistry, Chemical Engineering and Biotechnology, Nanyang Technological University, 62 Nanyang Drive, 637459, Singapore

ARTICLE INFO

Keywords:
brewers' spent grains
Emulsions
Proteins
Fibres
Pickering particles

ABSTRACT

The sustainable production of food ingredients can be achieved by utilising waste streams, but it is difficult to isolate pure components from a heterogeneous matrix. In this work, brewers' spent grains (BSG), which is a by-product from the brewing industry, was mildly treated with a colloid mill and its emulsifying ability was evaluated. The milled samples contained 26–32% protein and 52–62% fibre and were generally smaller than 10 μm. In its soluble fraction, a small amount of surface-active proteins was present and reduced oil-water interfacial tension by 35%. Emulsions prepared with the milled BSG and its insoluble particles were stable against coalescence for 10 days, with respective droplet sizes of 40 μm and 25 μm. The presence of fibres caused droplet flocculation but also helped to promote network formation. Our results suggest that obtaining pure components may not be necessary for emulsification purposes, especially for the case of particle-stabilised emulsions.

Industrial relevance: Industrial by-products from food processing are generated in large quantities and typically discarded due to their recalcitrant nature. Yet, there is more that can be exploited from this waste stream including proteins and fibres. Separation of these components in their purified form would require harsh methods that are not environmentally sustainable. This study provided insights into the use of a mild and scalable process that can produce functionally active dispersions that are of interest in the preparation of emulsions.

1. Introduction

Every year, 39 million tonnes of brewers' spent grains (BSG) are generated around the world as a side stream of the brewing industry (Macias-Garbett, Serna-Hernández, Sosa-Hernández, & Parra-Saldívar, 2021). BSG makes up 85% of the total byproducts from the brewing industry and is produced after the malting and mashing process, during which starch in barley grains is converted into soluble sugars. This leaves behind the original barley grain coverings, such as the pericarp, husk and aleurone layers which are rich in fibres and proteins. As a largely water-insoluble material with a high moisture content, BSG is highly susceptible to microbial contamination and most BSG is currently discarded or used as animal feed. BSG fibres comprise of 17% cellulose, 28% hemicellulose and 28% lignin, while the proteins, which make up 20% of the material, are mostly alcohol-soluble prolamins and alkali-soluble glutelins that remain in the barley grains (Mussatto, Dragone, & Roberto, 2006). These proteins have a good balance of hydrophobic and hydrophilic amino acids, which should allow them to exhibit good emulsifying properties (Wang et al., 2010).

Various methods to put BSG to valuable use have been explored, including the extraction of BSG fibres and proteins under alkaline conditions (Connolly, Piggott, & FitzGerald, 2013; Vieira et al., 2014). In particular, the enzymatic hydrolysis of BSG has been widely investigated to generate protein hydrolysates that have better technofunctional and bioactive properties (Celus, Brijs, & Delcour, 2007; Connolly et al., 2019; Niemi, Martins, Buchert, & Faulds, 2013). However, these fractionation processes often involve intensive physicochemical and thermal steps, the use of harsh solvents or end in large mass losses. In addition, previous studies have demonstrated that mildly purified mixtures can also be functional, depending on their intended application (Karefyllakis, Octaviana, van der Goot, & Nikiforidis, 2019; Möller, van der Padt, & van der Goot, 2022; Sridharan, Meinders, Bitter, & Nikiforidis,

* Corresponding author.
E-mail addresses: yiling002@e.ntu.edu.sg (Y.L. Chin), taghiandinani@gmail.com (S.T. Dinani), wnchen@ntu.edu.sg (W.N. Chen), remko.boom@wur.nl (R. Boom).

https://doi.org/10.1016/j.ifset.2023.103541
Received 23 August 2023; Received in revised form 24 November 2023; Accepted 30 November 2023
Available online 6 December 2023

2020), thus complex purification steps may in fact not be necessary. A straightforward and more sustainable approach is to utilise BSG as such. One example is the direct incorporation of BSG 'as is' in food products such as baked goods, pasta or yogurt, with the purpose of improving the dietary fibre content in the final application (Mussatto, 2014). Being a nutrient-rich material, BSG was also used as a substrate for growing microorganisms to produce industrially relevant compounds (Lynch, Steffen, & Arendt, 2016), or by employing microbes to break down the lignocellulosic structure and produce other useful components (Chin, Chai, & Chen, 2022; Cooray & Chen, 2018; Tan, Mok, & Chen, 2020).

However, until now, little attention has been paid towards physical modifications that could impart new or better functional properties to the whole BSG material. A recent study by Ibbett, White, Tucker, and Foster (2019) showed that colloid milling of BSG produced a protein-rich, fine dispersion with the ability to stabilise oil-in-water emulsions, but the interfacial properties and emulsifying behaviour were not investigated in further detail. In addition, only the proteins in BSG were considered for its potential to stabilise emulsions, neglecting the possibility that fibres could also have an effect on emulsification and emulsion stability. Previous studies have shown that insoluble fibres that are pretreated via a homogenisation step can possess emulsifying properties and stabilise emulsions through a combination of Pickering stabilisation and the formation of a fibre-based network (Bao et al., 2021; Wallecan, McCrae, Debon, Dong, & Mazoyer, 2015; Yang, Liu, Li, & Tang, 2019). The homogenisation process disrupts the plant cell wall matrix and can be carried out by high pressure homogenisation, ultrasonication or wet media milling. Emulsions stabilised by these fibres have demonstrated high stability against pH and ionic strength variations, with long-term storage stability. Similarly, water-insoluble proteins from corn and pea have also demonstrated to be effective particle stabilisers of oil-in-water emulsions (de Folter, van Ruijven, & Velikov, 2012; Hinderink, Schröder, Sagis, Schroën, & Berton-Carabin, 2021).

In recent years, substantial interest in clean-label and sustainable products has led to extensive research on particle-stabilised emulsions, i.e. Pickering emulsions, mainly due to their high physical stability (Schröder, Laguerre, Tenon, Schroën, & Berton-Carabin, 2021). For these reasons, it is relevant to consider exploiting the insolubility of BSG for Pickering stabilisation. We hypothesise that as a mixture containing amphiphilic proteins and a large amount of fibres, BSG can be used to stabilise emulsions without isolation of pure components. Therefore, the aim of this study is to characterise colloid mill-treated BSG and investigate the emulsifying ability of BSG as a whole and more specifically of its insoluble fraction. In this work, BSG was first treated with a colloid mill and separated by centrifugation to obtain an insoluble pellet fraction (insoluble BSG). The composition, physical behaviour, particle size and morphology of full and insoluble BSG dispersions were evaluated while the interfacial properties of the soluble component from centrifugation was determined. Emulsions were prepared with full and insoluble BSG and assessed based on their droplet sizes, charges, protein surface load, microstructure and creaming stability.

2. Materials and methods

2.1. Materials

BSG was kindly supplied by Heineken Nederland B.V. (The Netherlands). Hexane was purchased from Actu-All Chemicals B.V. (The Netherlands). Soybean oil was purchased from a local supermarket (The Netherlands). Sodium dodecyl sulfate (SDS) was purchased from Sigma-Aldrich (USA). Calcofluor White and Fast Green FCF were purchased from Sigma-Aldrich (USA). BODIPY™ 493/503 was purchased from Thermo Fisher Scientific (USA). All other reagents were purchased from Sigma-Aldrich (USA) unless otherwise stated. For all experiments, Milli-Q water was used.

2.2. Preparation of BSG for colloid milling

Wet BSG was dried in a fluidised bed dryer (TG200, Retsch GmbH, Germany) at 55 °C for 3 h in batches using an airflow of 70 m^3/h. The dried BSG (moisture content <4%) was impact-milled (Multimill, Hosokawa Alpine, Germany) with the ZPS configuration at 7000 rpm and a classifier wheel speed of 2500 rpm. Air flow was fixed at 52 m^3/h and feed rate was 3 kg/h. Milled BSG was then passed through a 100 μm air-jet sieve (e200LS, Hosokawa Alpine, Germany).

2.3. Preparation of full BSG and insoluble BSG dispersions

BSG (< 100 μm) was dispersed in water (2 wt%) and magnetically stirred at 600 rpm for 30 min at room temperature. The dispersion was colloid milled (magic LAB, IKA, Germany) at 20,000 rpm for 60 min using the MK module set at a gap size of 0.159 mm. To prepare the insoluble BSG, full BSG was centrifuged at 10,000 *g* for 10 min at 20 °C. The pellet was collected and freeze-dried (Epsilon 2-10D LSCplus, Martin Christ, Germany).

2.4. Compositional analysis

The nitrogen content was determined by the Dumas combustion method (FlashSmart™ Elemental Analyzer, Thermo Scientific, US), with a protein conversion factor of 5.83 (Jones, 1931). The lipid content was determined using hexane in a SOXTHERM® unit. The ash content was determined by gravimetric method in a furnace at 550 °C for 24 h (AAF1100, Carbolite, UK). The fibre content was determined by difference.

2.5. Microscopy, particle size and morphology

The aggregation behaviour of particles in aqueous media and the microstructure of emulsions were observed by light microscopy using a Carl Zeiss Axioscope A1 microscopy equipped with a camera (Axiocam 305 colour). Particle size measurements and morphology were performed by automated imaging (Morphologi 4, Malvern Instruments, UK) with at least 100,000 particles measured each time and estimated as a circle-equivalent diameter. Dried particles were also visualised using a scanning electron microscope (JCM-7000 NeoScope™ Benchtop SEM, JEOL, Japan). Emulsions were observed by confocal laser scanning microscopy using a ReScan Confocal Microscope (Confocal.nl, The Netherlands) fitted with a 60× water objective and a camera. Samples were simultaneously stained with Calcofluor White, Fast Green FCF and BODIPY™ for the fibres, proteins and oil phase, respectively. BODIPY™ was dissolved in ethanol, while the other two stains were dissolved in water. The emission wavelengths used were 405, 488 and 640 nm for Calcofluor White, BODIPY™ and Fast Green FCF respectively.

2.6. Interfacial tension and dilatational rheology

The interfacial tension between stripped soybean oil and the soluble filtered fraction (< 0.2 μm) of the supernatant was measured using an automated drop tensiometer (Tracker, Teclis Scientific, France) used in the rising drop configuration. An oil droplet with a surface area of 30 mm^2 was formed at the tip of a stainless steel needle immersed in the dispersion at 20 °C. The shape of the oil droplet was continuously monitored using a camera and transformed into interfacial tension by Wdrop® software (Teclis Scientific, France). The interfacial tension reached a steady value after 3 h and the dilatational viscoelasticity was measured using an amplitude sweep test. The droplet was subjected to sinusoidal amplitude deformations that varied its projection area by 5%, 10%, 15%, 20%, 25%, 30%. The interfacial tension was recorded as a function of time together with the amplitude and phase shift of the deformation. These measurements were used to estimate the interfacial dilatational modulus (E_d), which is a measure of the resistance to surface

disturbances and can be defined as $E_d = E_d^{'} + E_d^{''}$, with $E_d^{'}$ and $E_d^{''}$ referring to the storage and loss modulus respectively, obtained from the amplitude sweep tests. Additional experiments pertaining to the identification and quantitation of proteins in the soluble filtered fraction were also performed using Fourier-Transform Infrared Spectroscopy (FTIR) and a bicinchoninic acid assay (Thermo Fisher Scientific, USA).

2.7. Emulsion preparation

Full BSG dispersions were diluted with Milli-Q water and lyophilised insoluble BSG was re-dispersed in water. Soybean oil (10 wt%) was added to an aqueous phase (90 wt%) containing 0.5, 1 or 2 wt% of particles. A coarse emulsion was prepared using a rotor-stator homogeniser (Ultra Turrax T18 Digital, IKA, Germany) at 11,000 rpm for 2 min. Subsequently, the emulsion was processed with an ultrasonic probe (Branson Digital Sonifier SFX 550, Emerson, USA) using a 5 mm probe at 70% amplitude for 5 min (3 s on/3 s off). Emulsions were immersed in an ice bath to prevent excessive heating. At least two emulsions were prepared independently for each measurement.

2.8. Emulsion droplet size

Droplet size measurements were performed by laser light diffraction (Mastersizer 3000, Malvern Instruments, UK) using the Hydro MV module. A refractive index of 1.468 for the dispersed phase with an absorption index of 0.01 were used. For measurements with SDS, 1% SDS was diluted with the sample in a 1:1 ratio. Each measurement was performed in triplicate on days 0, 5 and 10.

2.9. Zeta potential of emulsions

The surface charge of the emulsion droplets was measured by dynamic light scattering (Zetasizer Ultra, Malvern Instruments, UK) using a Malvern folded cuvette (DTS1070) at 25 °C. Before measurement, the emulsion samples were diluted 500 times in Milli-Q water to prevent multiple scattering. Each measurement was performed in triplicate.

2.10. Protein surface load of oil droplets

The protein surface load of oil droplets was determined in accordance to Sridharan et al. (2020) with slight modifications. The prepared emulsions were centrifuged at 10,000 *g* for 30 min at 4 °C and subsequently stored at -20 °C for overnight. The cream layer was carefully separated from the frozen serum and dried in the oven at 60 °C for 48 h. The protein content in the dried cream layer was determined by Dumas as mentioned in section 2.4. Protein surface load (Γ_S, in mg/m^2) was computed by Eqs. 1a and 1b.

$$\Gamma_S = \Gamma_T / S_T \tag{1a}$$

$$S_T = 6V_{oil}/d_{32} \tag{1b}$$

Where Γ_T is the measured amount of protein at the interface, S_T is the total surface area, d_{32} is the surface mean diameter from laser diffraction experiments and V_{oil} is the volume of oil in the emulsion.

2.11. Creaming index

As the emulsions prepared with 2 wt% dispersions had the smallest droplet sizes, the storage stability of these emulsions against creaming was evaluated. Emulsions were stored at 4 °C and creaming was determined by recording the total height of the emulsion (Ht) and the height of the transparent or turbid layer at the bottom of the container (Hs) on days 0, 3, 5, 8 and 10. The creaming index was calculated using Eq. 2.

$$\text{Creaming index } (\%) = Hs/Ht \times 100\% \tag{2}$$

2.12. Statistical analysis

All experimental data were analysed using SPSS Statistical Software (Version 28, IBM, US). Significant differences were analysed with one-way ANOVA using a descriptive Duncan's test at a significant level of 95% ($P \leq 0.05$). All experiments were done at least in duplicate and reported results are shown as mean ± standard deviation.

3. Results and discussion

3.1. Characterisation of particle dispersions

3.1.1. Composition of mixtures

The effects of colloid milling and subsequent centrifugation on the composition of BSG were compared as shown in Table 1. The main components in the initial BSG comprised of proteins and fibres, which is in line with those previously reported (Lynch et al., 2016; Mussatto et al., 2006). Colloid milling was used as a physical treatment to reduce particle size as large particles will sediment quickly and are less likely to exert any stabilising effects on an oil-water interface. After colloid milling, the protein content in full BSG remained the same as the initial BSG while there was a slight increase in the lipid content ($P \leq 0.05$), probably because colloid milling released some oil bodies from the endosperm, embryo and aleurone layer of the barley grain (Neuberger et al., 2008; Niemi et al., 2012). Following centrifugation, the protein and lipid content decreased in the insoluble BSG while the fibre content increased. It was previously reported by Ibbett et al. (2019) that after colloid milling and centrifugation, an upper fine fraction that is richer in proteins and lipids relative to the initial BSG was generated. As a result of colloid milling, protein-containing tissues are broken into smaller fragments and the smaller protein-containing particles sediment more slowly than the larger husk or pericarp particles upon centrifugation. Since lipids and proteins are also components of protein bodies in barley (Becker, 2007), it is therefore likely that the supernatant which is more enriched in proteins would also have an improvement in lipid content, thus the remaining insoluble BSG pellet would have lesser proteins and lipids. Overall, despite the minor differences in the composition of full BSG and insoluble BSG, the distribution of components remained relatively similar, in which proteins and fibres make up the bulk of the material. It is also worth mentioning that in this study, BSG was dried before colloid milling to ensure stability of the material against microbial degradation. However, in reality, BSG is already in a wet state after brewing, and it would be more practical to directly process it in the colloid mill immediately after brewing. This would help to save costs involved in drying.

3.1.2. Physical behaviour, particle size and morphology

Following the compositional analysis, the dispersibility and aggregation behaviour of full BSG and insoluble BSG in water was investigated. The dispersions were well suspended immediately after homogenisation, but showed moderate aggregation when observed under the light microscope (Fig. 1). This could be associated to flocculation caused by fibres or may suggest that the particles are somewhat

Table 1
Composition of BSG before and after colloid milling and the remaining pellet after centrifugation. Fibre was calculated from the other components by mass balance. Different small upper letters in the same row indicate significant difference at $P \leq 0.05$.

Composition (%)	Initial BSG before colloid milling	Colloid-milled BSG (Full BSG)	Pellet after centrifugation (Insoluble BSG)
Protein	31.4 ± 0.5 ^{a}	31.6 ± 0.9 ^{a}	25.8 ± 2.1 ^{b}
Lipids	12.8 ± 0.5 ^{b}	14.6 ± 0.4 ^{a}	8.8 ± 0.4 ^{c}
Ash	3.7 ± 0.09 ^{a}	2.4 ± 0.004 ^{c}	3.1 ± 0.09 ^{b}
Fibre	52.1	51.5	62.3

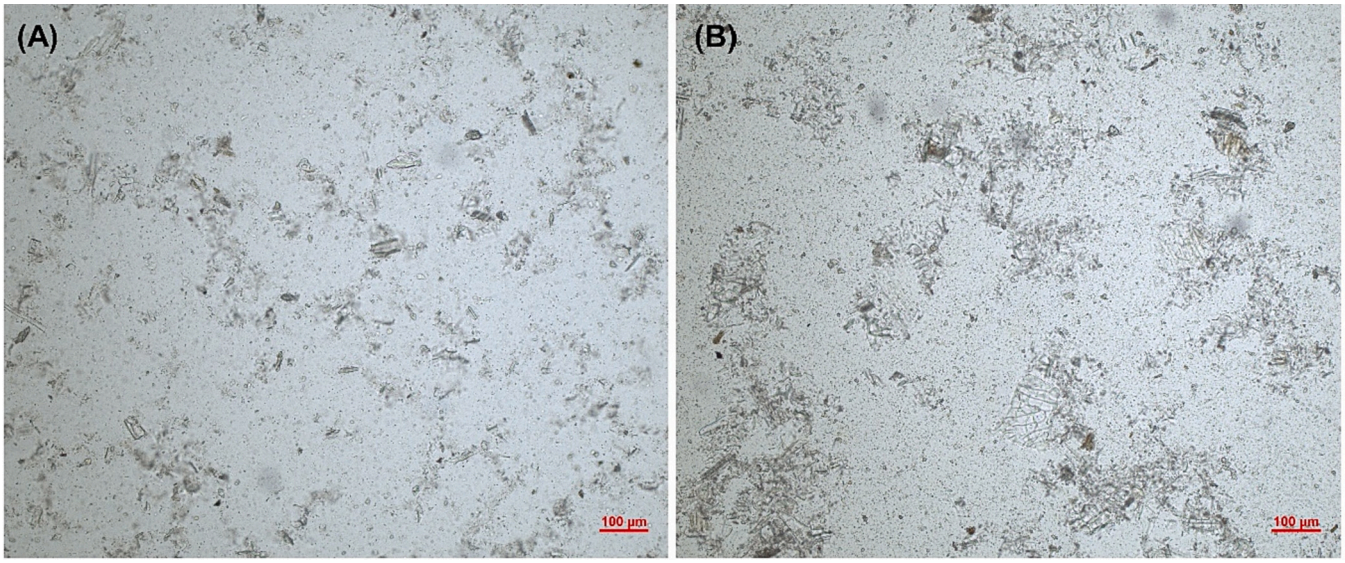

Fig. 1. Particle dispersion of (A) full BSG and (B) insoluble BSG under the light microscope after homogenisation. Scale bar represents 100 µm.

hydrophobic, which may indicate their suitability for forming stable Pickering oil-in-water emulsions (Binks, Rodrigues, & Frith, 2007).

The particle size distributions of the homogenized dispersions of full BSG and insoluble BSG are depicted in Fig. 2. Taking into account the particle shape, both dispersions had an asymmetric particle size distribution, with majority of the particles having a circle-equivalent diameter below 10 µm. From the particle size distribution, there are more particles below 1 µm in full BSG than insoluble BSG, which can be attributed to the generation of fine particles after colloid milling followed by the removal of some fines in insoluble BSG after centrifugation. This is in agreement with Ibbett et al. (2019) who obtained fine particles in the supernatant around 1–10 µm in size after colloid milling and centrifugation on BSG and found that the fine particles were rich in proteins with the ability to stabilise oil-in-water emulsions. Pickering particles that are at least one order of magnitude smaller than the targeted emulsion droplet size generally provide good surface coverage and can give effective Pickering stabilisation (Schulman & Leja, 1954). However, it is also possible to make stable emulsions comprising of oil droplets that are similar in size as the particles in dispersion, as demonstrated by Gould, Vieira, and Wolf (2013) and Kurukji, Pichot, Spyropoulos, and Norton (2013) using cocoa particles, since only the finest particles stabilise the emulsion. Given that majority of the particles in this study are below 10 µm, we hypothesised that stable emulsions can be produced.

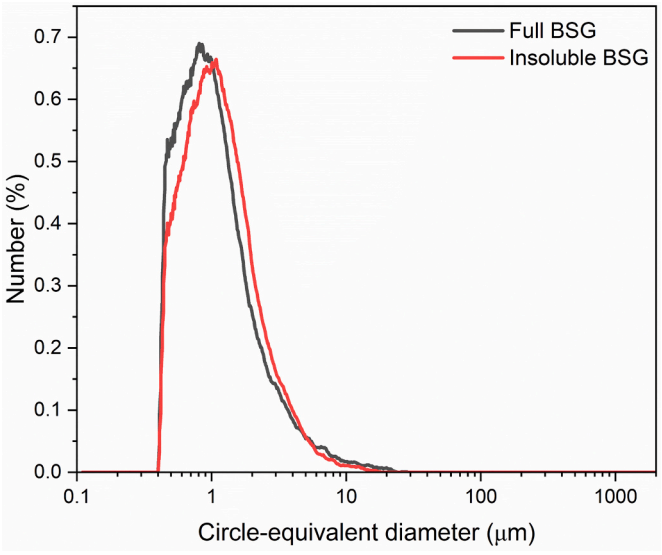

Fig. 2. Particle size distribution of dispersions made from full BSG and insoluble BSG after homogenisation.

As the shape of the particles will influence their interfacial behaviour and their ability to stabilise interfaces (Berton-Carabin & Schroen, 2015), the morphology of the particles was examined in their dried form using SEM and as a homogenized dispersion using automated imaging analysis. The SEM images show that both particles have an irregular, uneven surface (Fig. 3). The elongation, defined as $\left(1-\frac{width\ of\ particle}{length\ of\ particle}\right)$, was 0.32 ± 0.01 and 0.33 ± 0.03 for full BSG and insoluble BSG dispersions respectively. This implies that both samples had particles with an anisotropic shape which could be related to the presence of the fibres and makes it possible to cover a higher fraction of the interfacial area by inducing the formation of a network-like structure at the emulsion droplet surface through jamming. Additionally, the adsorption of an anisotropic particle is stronger than for a spherical particle as the interfacial area-to-particle size ratio is larger, which helps to prevent coalescence (Madivala, Vandebril, Fransaer, & Vermant, 2009).

3.1.3. *Interfacial tension and dilatational rheology*

In previous studies, colloid milling was found to disintegrate the physical structure of fibres and result in an increase in soluble components (Ullah et al., 2018). These soluble components may be surface-active and have an effect on the interfacial behaviour. On the other hand, the adsorption of insoluble particles at the interface in the case of a particle-stabilised emulsion does not influence the interfacial tension (Vignati, Piazza, & Lockhart, 2003). Therefore, the interfacial tension informs us on the type of components that are present. As such, the supernatant obtained after centrifugation was filtered and the droplet interfacial tension was measured over time as illustrated in Fig. 4A.

The interfacial tension between stripped soybean oil and water without any BSG addition was around 31 mN/m and remained stable over the timescale of the experiment. The soluble components in the supernatant gradually decreased the interfacial tension and reached about 20 mN/m after 3 h. To verify whether soluble proteins could be the cause for the reduction of the interfacial tension, FTIR was used to identify bands in the amide I and II region (1500–1700 cm^{-1}) that are typical of proteins (Supplementary Information, Fig. 1). A bicinchoninic acid assay was also performed to estimate the protein content present. The results suggest that proteins with a concentration of 0.2 ± 0.02 mg/

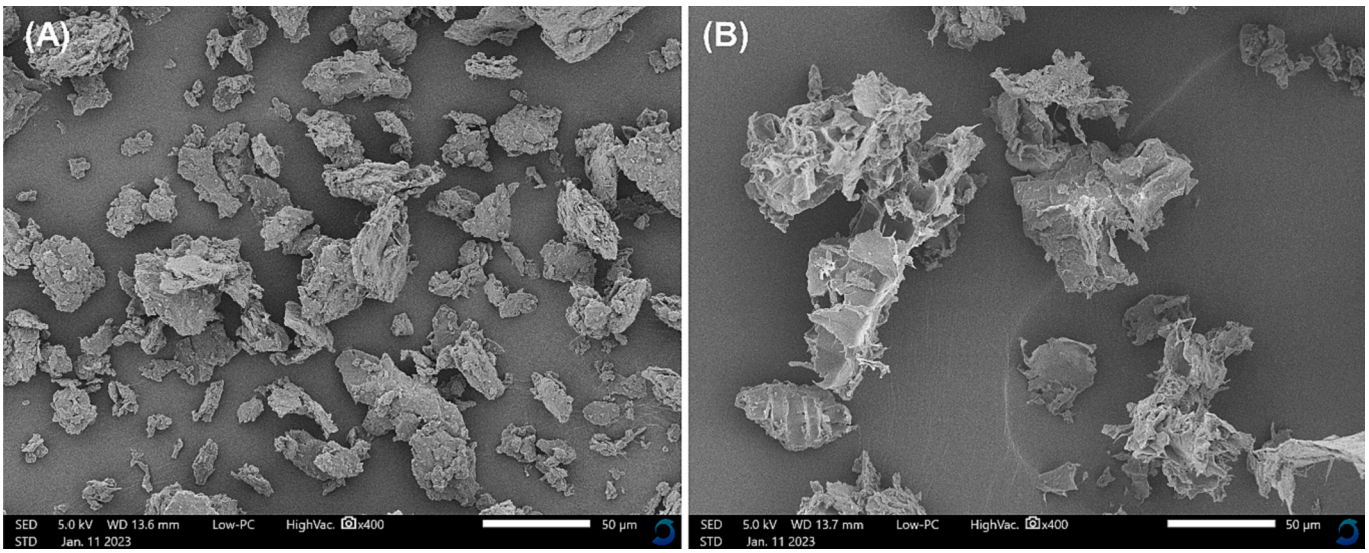

Fig. 3. SEM images of the dispersion of (A) full BSG and (B) insoluble BSG. Scale bar represents 50 µm.

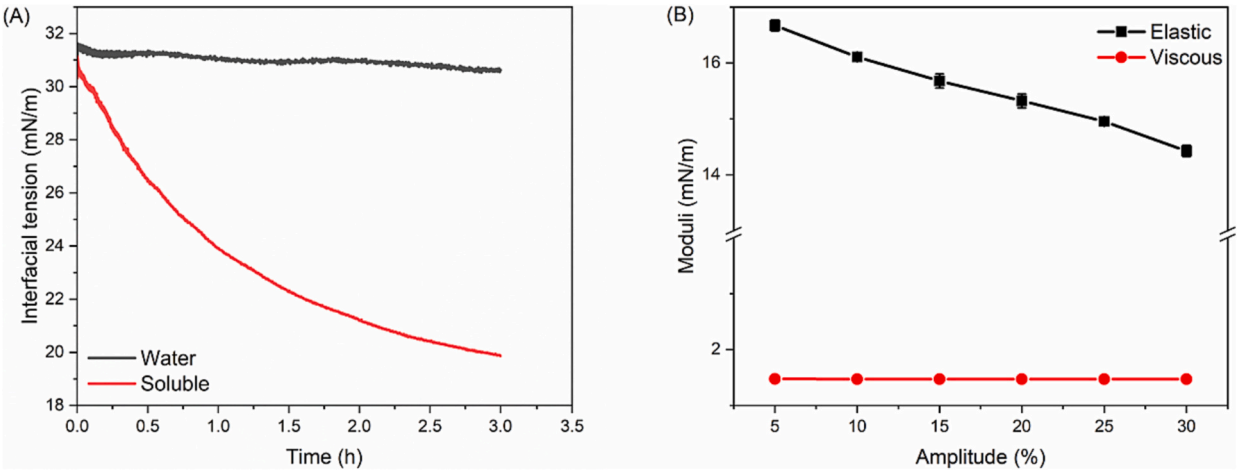

Fig. 4. (A) Interfacial tension of oil-water interface stabilised by the soluble component in the supernatant as a function of time; (B) Dilatational elastic and viscous modulus of soluble component in the supernatant as a function of amplitude of droplet deformation.

ml were indeed present in the soluble fraction, which could arise from residual wort proteins remaining in the BSG after lautering (Celus, Brijs, & Delcour, 2006) or from the release of soluble proteins as a result of colloid milling (Anderson & Guraya, 2001).

Apart from the ability to reduce the interfacial tension, the viscoelasticity of the interface formed by the soluble fraction of the supernatant was examined by dilatational rheology (Fig. 4B). The elastic modulus (14–17 mN/m) was much higher than viscous modulus (~1.5 mN/m), indicating predominantly elastic behaviour, which is characteristic of protein adsorption at the interface (Evans, Ratcliffe, & Williams, 2013). In the case of full BSG where soluble proteins exist together with insoluble particles, soluble proteins can compete with particles to adsorb at the interface. It is also possible that the soluble proteins reduce the interfacial tension to an extent that the high desorption energy for particles is lowered and adsorbed particles on the interface are displaced, as observed by Vashisth, Whitby, Fornasiero, and Ralston (2010) between silica nanoparticles and SDS.

3.2. Characterisation of emulsion and its physical stability over time

3.2.1. Droplet size

Oil-in-water emulsions (10 wt%) were prepared with full BSG and insoluble BSG at concentrations of 0.5, 1 and 2 wt% in the aqueous phase. The emulsion droplet size was determined to investigate the emulsifying ability of these multicomponent mixtures. Both light microscopy and laser diffraction were used to estimate the actual droplet size as non-adsorbed particles could also contribute to the scattered light signal. Based on light microscopy images without SDS added (Fig. 5), the individual emulsion droplet sizes of fresh emulsions prepared with full BSG and insoluble BSG were estimated to be 40 µm and 25 µm respectively. As expected, the large particle sizes present in the dispersions contributed to the large droplet sizes of both emulsions. Both emulsions also showed network formation in the continuous phase, which could be due to particle bridging or flocculation. To determine whether flocculation occurred, SDS was used as an anionic detergent to disrupt hydrogen bonds that developed among proteins and other dispersed components. Full BSG emulsions diluted with SDS showed more well-dispersed droplets in the continuous phase, indeed indicating reversible flocculation of the droplets, which is probably due to interactions between soluble proteins. On the other hand, clusters of droplets were still seen in the insoluble BSG emulsion, which may suggest that particle bridging was more dominant here, since particle adsorption to the oil-water interface is not likely to be affected by SDS. The differences in droplet sizes and aggregated states of emulsions prepared with full BSG

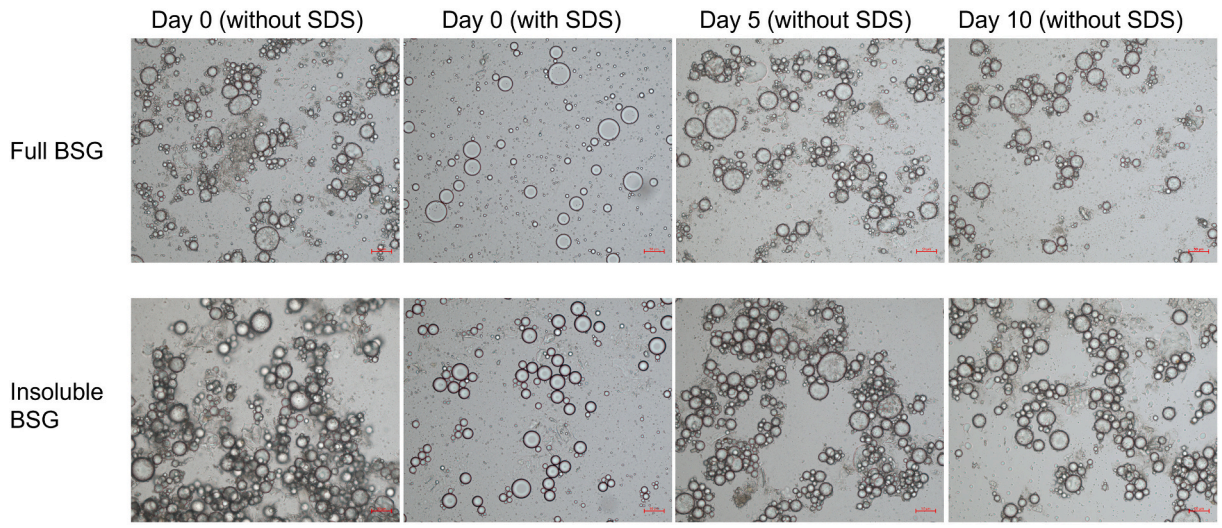

Fig. 5. Light micrographs of emulsions prepared with full BSG and insoluble BSG prepared at 2 wt% at day 0, 5, 10. Scale bar represents 50 μm.

and insoluble BSG could be attributed to the presence of surface-active proteins in the full BSG. Studies have shown that multicomponent systems that contain surface-active molecules, as in the case of full BSG, may compete with particle adsorption at the oil-water interface, and result in incomplete surface coverage that leads to larger emulsion droplets. Surface-active molecules could also adsorb onto particles and induce flocculation (Berton-Carabin & Schroen, 2015). Nonetheless, over time, the emulsion droplet sizes remained relatively constant based on microscopic observations, indicating that minimal coalescence of droplets occurred during storage.

The droplet size distribution of both emulsions was also investigated with laser light diffraction. From Fig. 6, both emulsions displayed a similar polydisperse distribution, except for a large proportion of droplets above 100 μm in full BSG, which could suggest flocculation or coalescence. When SDS was added to the emulsions, there was a reduction in droplet size above 100 μm in full BSG, indicative of flocs that were broken up by SDS, which was not observed with insoluble BSG. This implies that some droplets were flocculated in full BSG which could be due to weak electrostatic repulsion or the presence of surface-active components that compete with the particles for adsorption. Since oil droplets of insoluble BSG are stabilised solely by particles, the interfacial thickness is expected to be at least equal to the size of particles. On the other hand, the presence of soluble proteins in full BSG may interfere with the adsorption of particles on the oil-water interface and reduce the interfacial thickness. Therefore, a thicker interfacial region in insoluble BSG may also contribute to the absence of flocs. Over time, the droplet sizes (d_{32}) of both emulsions did not change significantly over time ($P \leq 0.05$), which is in line with the light microscope images that the emulsion remained physically stable during storage.

The concentration of particles also influenced the size of the emulsion droplets. Irrespective of the dispersion used, increasing the particle concentration shifted the size distribution to the left (Fig. 7), since more particles were present to stabilise the extra oil-water interface required for smaller droplets. However, we can observe that at 2 wt% particle concentration, the distribution becomes trimodal. The peak at the smaller size range could refer to the emulsion droplets in the system while the peak at the larger size range could be related to the higher degree of flocculation in the system. Other studies also suggested the possible formation of a fibre-based network among oil droplets at higher particle concentration (Qi, Song, Zeng, & Liao, 2021), which could also be perceived as the presence of a large aggregate in the emulsion.

3.2.2. *Zeta-potential*

The zeta potential is a measure of the surface charges present on the oil droplets, which is an indicator of colloidal stability. All emulsions had a negative charge, with an initial zeta potential of about −28 mV and − 26 mV for full BSG and insoluble BSG emulsion respectively (Fig. 8). There was no significant difference ($P > 0.05$) in the surface

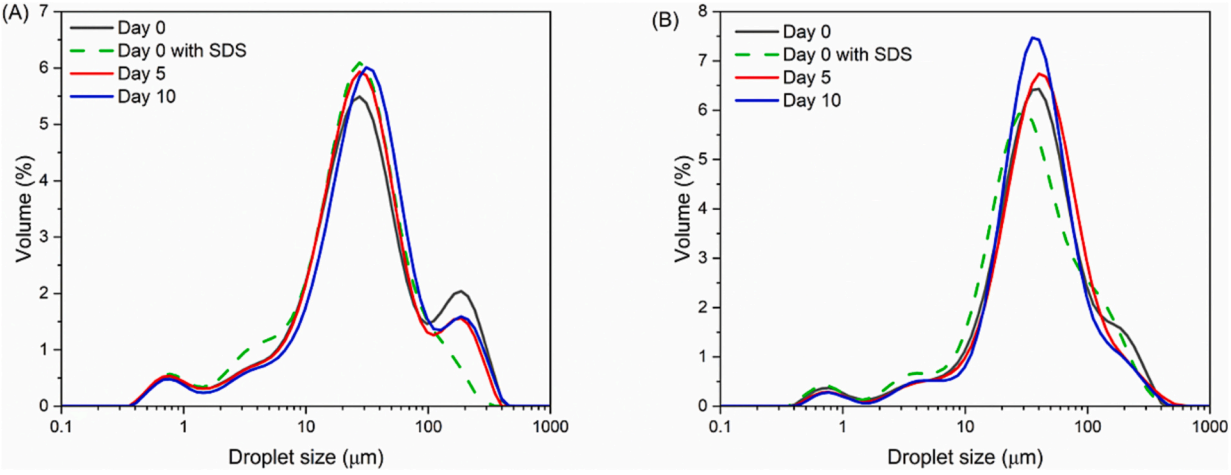

Fig. 6. Emulsion droplet size distribution of 2 wt% (A) full BSG and (B) insoluble BSG over time.

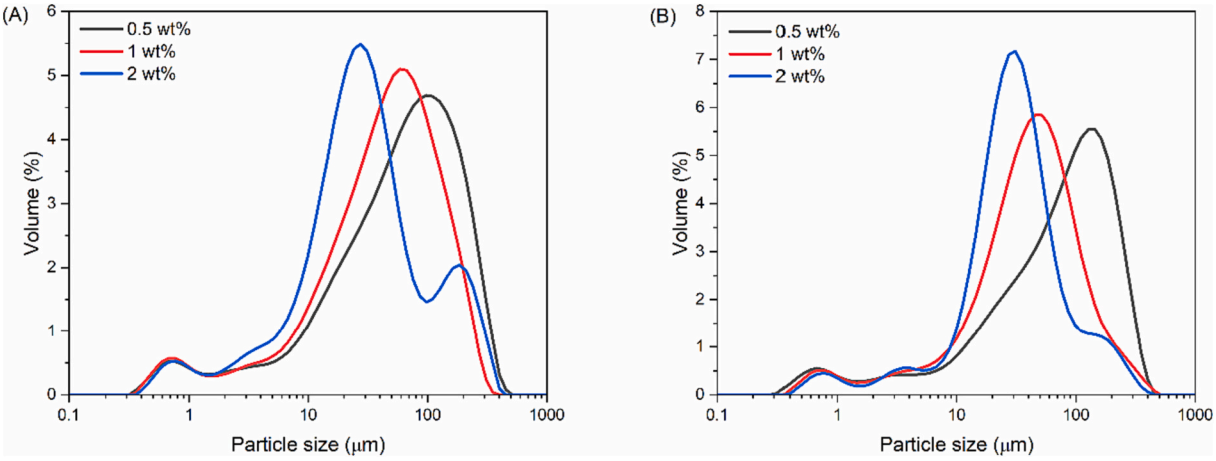

Fig. 7. Emulsion droplet size distribution of (A) full BSG and (B) insoluble BSG with particle concentration of 0.5, 1, 2 wt% at day 0.

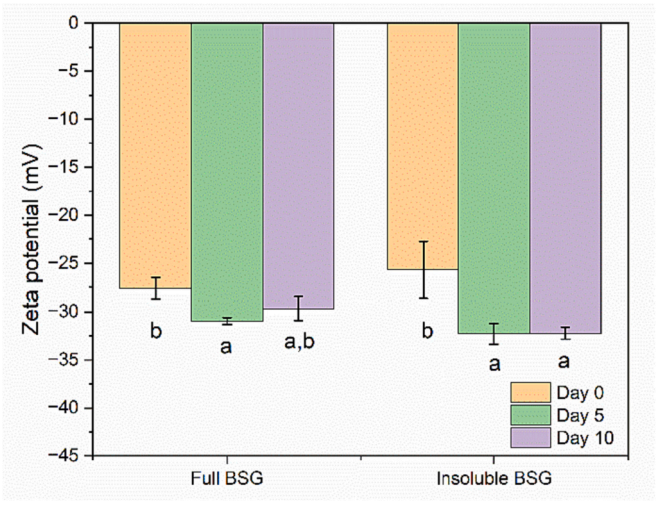

Fig. 8. Zeta potential of emulsions prepared with full BSG and insoluble BSG at 0.5 wt% in aqueous phase over time. Different small letters in the same sample indicate significant difference at $P \leq 0.05$. Error bars refer to standard deviations.

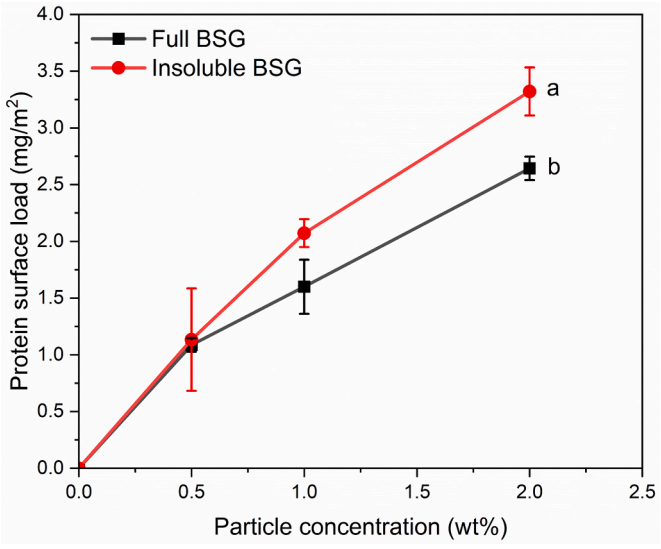

Fig. 9. Protein surface load as a function of particle concentration for full BSG and insoluble BSG. Different small letters indicate significant difference at $P \leq 0.05$. Error bars refer to standard deviations.

charge between full BSG and insoluble BSG across all days. These net zeta potentials are higher than those of emulsions stabilised with full and insoluble pea proteins with values of −16 mV and − 18 mV respectively (Hinderink et al., 2021). This could indicate a contribution of negative charges by the fibres (Sjostrom, 1989). Over time, there was a slight increase in the net zeta potential (more negatively charged) which could be due to conformational rearrangement of the proteins at the interface (Wiącek & Chibowski, 2002). With this surface charge, emulsion droplets are likely to experience strong electrostatic repulsion (Freitas & Müller, 1998). However, the presence of non-adsorbed biopolymers could lead to depletion forces, while fibres that adsorb on the interface could bridge oil droplets (Dickinson, 2009). Both phenomena result in oil droplet flocculation, as observed in Fig. 5.

3.2.3. *Protein surface load*

The protein surface load of the emulsions was determined to examine whether the amount of proteins adsorbed at the interface was influenced by the choice of dispersion (Fig. 9). In both emulsions, a higher particle concentration, which translates to an increase in protein concentration, led to enhanced hydrophobic interactions between adsorbed proteins and more protein adsorption at the interface. At low particle concentrations, there was no significant difference in protein surface load between full BSG and insoluble BSG, presumably due to less soluble proteins present, thereby enabling sufficient time for particles to adsorb. However, at 2 wt% particle concentration, full BSG had a significantly lower protein surface load ($P \leq 0.05$) than insoluble BSG despite the higher protein content in full BSG (Table 1). We attribute this to the competitive adsorption between soluble proteins and particles in full BSG that prevents complete interface coverage, resulting in larger emulsion droplets (Fig. 5). Considering that the interfacial thickness for particle-stabilised interfaces is at least equal to the particle size for a particle monolayer in particle-stabilised interfaces, the surface load is expected to be much larger as compared to conventional emulsifiers (Berton-Carabin & Schroen, 2015). The protein surface load of about 3.3 mg/m^2 obtained for insoluble BSG is extremely low when compared to an emulsion prepared with zein particles having a surface load of 109 mg/m^2 (Feng & Lee, 2016). This clearly suggests that there are insufficient protein particles adsorbed at the interface to sufficiently stabilise the emulsions. Yet, based on droplet sizes, the emulsions remained stable against coalescence, which suggests that non-protein particles, i.e. fibres, could have adsorbed on the interface and contributed to form a steric barrier that efficiently prevents droplet coalescence.

3.2.4. Microstructure of emulsions

To visualise the spatial arrangement of particles at the oil-water interface, confocal laser scanning microscopy was carried out. The confocal micrograph in Fig. 10 showed protein particles (red colour) surrounding oil droplets (green colour) and confirm that proteins adsorb at the oil-water interface, evident from the yellow spots produced from the combination of the green oil droplets and red protein on the interface. Fibre particles (blue colour) were found in the vicinity of the protein particles and oil droplets, suggesting that these particles might play a secondary role in stabilising (or bridging) the oil droplets. This is consistent with previous studies which suggest that proteins present on polysaccharide-rich materials could provide an amphiphilic surface that serve as an anchor on the oil-water interface (Dickinson, 2003; Wallecan et al., 2015). Therefore, while the presence of fibres may be favourable for stabilisation of the interface as they enable the formation of a network that facilitates particle adsorption at the interface or directly adsorb at the interface, they also induce bridging between droplets. These observations were seen in both emulsions prepared with full BSG and insoluble BSG, with smaller droplet sizes for the latter, as previously seen in section 3.2.1. Smaller droplet sizes provide larger interfacial surface area which contributes to emulsion stability.

3.2.5. Macroscopic behaviour of emulsions

The macroscopic behaviour of the emulsions was assessed by visual appearance and creaming stability measurements. Due to the large droplet sizes and the presence of flocs or aggregates in both emulsions, creaming of the emulsions was expected and evaluated by monitoring the creaming index. From Fig. 11A, the creaming index significantly increased over time ($P \leq 0.05$) and remained constant after day 8 in both emulsions. Between both samples, creaming was initially similar in both emulsions but after day 5, faster creaming was seen in the full BSG emulsion than the insoluble BSG emulsion ($P \leq 0.05$). This is associated to the larger emulsion droplets with the full BSG which indicates poorer emulsion stability. It is worth mentioning that after 10 days of storage, no free oil separation was observed for the emulsions, suggesting that no extensive coalescence occurred.

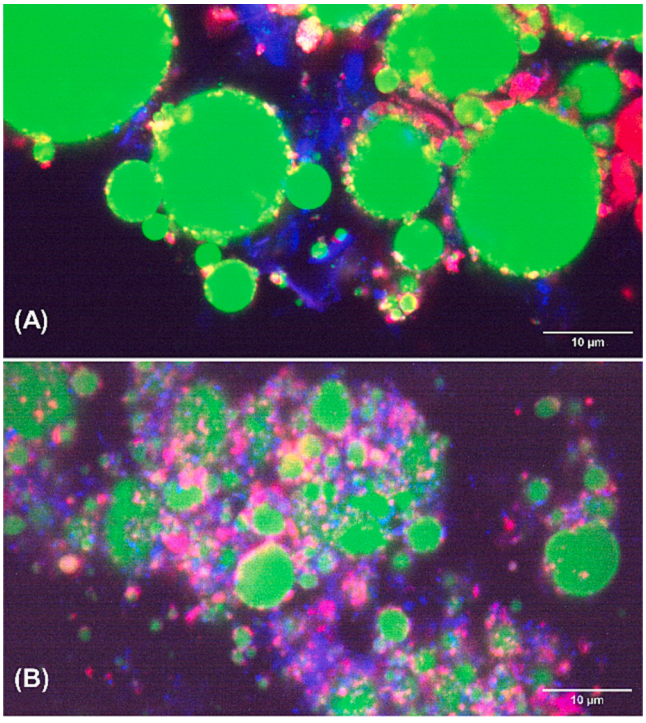

Fig. 10. CLSM micrograph of emulsions of (A) full BSG and (B) insoluble BSG. Lipids, fibres and proteins are coloured green, blue and red respectively. Scale bar represents 10 μm. (For interpretation of the references to colour in this figure legend, the reader is referred to the web version of this article.)

As presented in the photo of Fig. 11B, the emulsion was separated into two phases during storage, and this was observed in both emulsions. The top emulsion phase was a cream (brown) layer likely formed by large particle aggregates or droplet flocculation. The bottom phase, a white turbid layer, possibly contained small oil droplets that remained stable and were able to scatter light. According to Fig. 11B, as particle concentration increased, creaming was significantly reduced at 2 wt% ($P \leq 0.05$). We hypothesise that the particles need a certain minimum concentration to form a network around the oil droplets. When more particles are present in the continuous phase, network formation is promoted (Binks, 2002; Wallecan et al., 2015), therefore the upper layer is proportionally thicker. When there are sufficient BSG particles present, no creaming would occur. A correlation between particle concentration and the creaming index was determined to determine the minimum particle concentration required for no creaming to occur. Based on our calculations, emulsions prepared using full BSG or insoluble BSG as dispersions should contain a particle concentration of at least 3 wt% to ensure that creaming does not occur. This agrees with our results that there is insufficient protein (particles) on the emulsion droplets as visualised by CLSM and also discussed in section 3.2.3. An increase in particle concentration is likely to help stabilise the emulsions through the formation of a fibre-based network containing proteins adsorbed on the oil-water interface.

4. Conclusion

We investigated the emulsifying performance of mixtures obtained from brewers' spent grains after colloid milling. After physical treatment, full BSG and insoluble BSG were still largely composed of proteins and fibres and showed moderate aggregation in an aqueous dispersion. Oil-in-water emulsions prepared with full BSG showed reversible flocculation while the insoluble BSG formed particle bridges. Despite sufficient electrostatic repulsion between droplets, the presence of large amounts of fibres caused flocculation. Over a 10-day period, the emulsions prepared with full BSG and insoluble BSG did not show coalescence and were able to physically stabilise emulsions even with large droplet sizes, with the latter stabilised by a true Pickering mechanism while the former showed an antagonistic effect between soluble and insoluble parts of BSG. Microscopic observation suggests that insoluble BSG protein aggregates and their fibres are capable of stabilising emulsion droplets. Our findings suggest that mild processing of lignocellulosic waste materials rich in proteins and fibres can produce mixtures that have promising emulsifying performance and would comply with sustainable and clean-label strategies. After colloid milling, BSG can be used as a plant-based emulsifier without further purification. In addition, the presence of fibres also improve the nutritional quality of the emulsified product as it can serve as a prebiotic (Abdi & Joye, 2021).

CRediT authorship contribution statement

Yi Ling Chin: Conceptualization, Data curation, Formal analysis, Investigation, Methodology, Visualization, Writing – original draft. **Somayeh Taghian Dinani:** Supervision, Writing – review & editing. **Wei Ning Chen:** Project administration, Supervision. **Remko Boom:** Conceptualization, Project administration, Resources, Supervision, Writing – review & editing.

Declaration of Competing Interest

The authors declare that they have no known competing financial interests or personal relationships that could have appeared to influence the work reported in this paper.

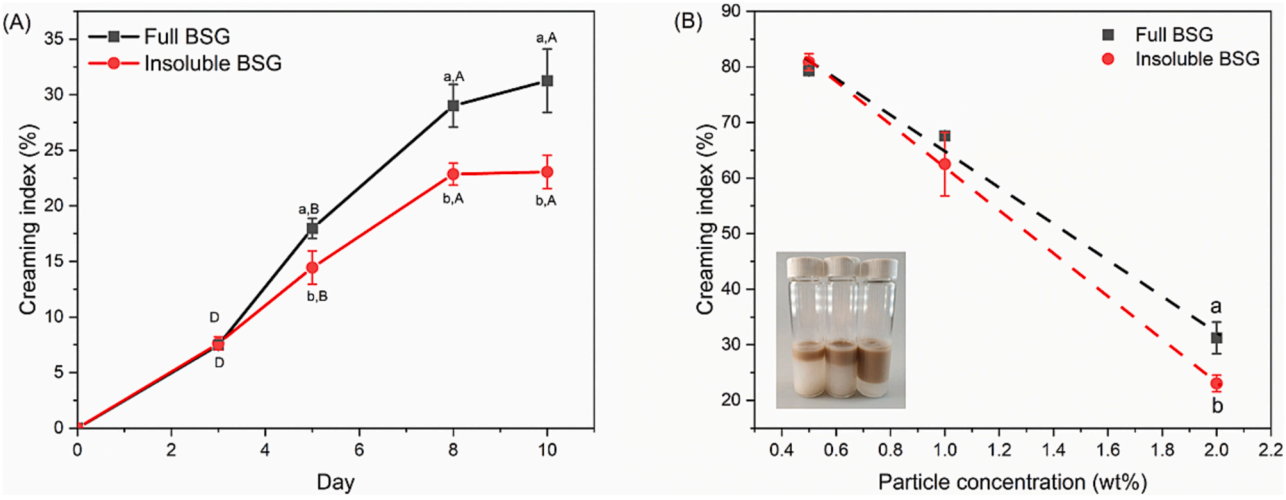

Fig. 11. (A) Creaming index of 2 wt% full BSG and insoluble BSG stored at 4 °C for 10 days; (B) Creaming index as a function of increasing particle concentration at day 10 (photo: an emulsion prepared with full BSG after 10 days, with increasing particle concentration from left to right). Different small letters indicate significant difference ($P \leq 0.05$) between full and insoluble BSG, and different big letters indicate significant difference ($P \leq 0.05$) between days. Error bars refer to standard deviations.

Data availability

Data will be made available on request.

Acknowledgements

The authors would like to acknowledge Wageningen University and Research and Nanyang Technological University for funding this research.

Appendix A. Supplementary data

Supplementary data to this article can be found online at https://doi.org/10.1016/j.ifset.2023.103541.

References

Abdi, R., & Joye, I. J. (2021). Prebiotic potential of cereal components. *Foods, 10*(10), 2338. https://www.mdpi.com/2304-8158/10/10/2338.

Anderson, A. K., & Guraya, H. S. (2001). Extractability of protein in physically processed rice bran. *Journal of the American Oil Chemists' Society, 78*(9), 969–972. https://doi.org/10.1007/s11746-001-0373-1

Bao, Y., Xue, H., Yue, Y., Wang, X., Yu, H., & Piao, C. (2021). Preparation and characterization of pickering emulsions with modified okara insoluble dietary fiber. *Foods, 10*(12), 2982. https://www.mdpi.com/2304-8158/10/12/2982.

Becker, R. (2007). Fatty acids in food cereal grains and grain products. In *Fatty acids in foods and their health implications* (pp. 317–330). CRC Press.

Berton-Carabin, C. C., & Schroen, K. (2015). Pickering emulsions for food applications: Background, trends, and challenges. *Annual Review of Food Science and Technology, 6*, 263–297. https://doi.org/10.1146/annurev-food-081114-110822

Binks, B. P. (2002). Particles as surfactants—Similarities and differences. *Current Opinion in Colloid & Interface Science, 7*(1), 21–41. https://doi.org/10.1016/S1359-0294(02)00008-0

Binks, B. P., Rodrigues, J. A., & Frith, W. J. (2007). Synergistic interaction in emulsions stabilized by a mixture of silica nanoparticles and cationic surfactant. *Langmuir, 23*(7), 3626–3636. https://doi.org/10.1021/la0634600

Celus, I., Brijs, K., & Delcour, J. A. (2006). The effects of malting and mashing on barley protein extractability. *Journal of Cereal Science, 44*(2), 203–211. https://doi.org/10.1016/j.jcs.2006.06.003

Celus, I., Brijs, K., & Delcour, J. A. (2007). Enzymatic hydrolysis of Brewers' spent grain proteins and Technofunctional properties of the resulting hydrolysates. *Journal of Agricultural and Food Chemistry, 55*(21), 8703–8710. https://doi.org/10.1021/jf071793c

Chin, Y. L., Chai, K. F., & Chen, W. N. (2022). Upcycling of brewers' spent grains via solid-state fermentation for the production of protein hydrolysates with antioxidant and techno-functional properties. *Food Chemistry: X, 13*, Article 100184. https://doi.org/10.1016/j.fochx.2021.100184

Connolly, A., Cermeño, M., Crowley, D., O'Callaghan, Y., O'Brien, N. M., & FitzGerald, R. J. (2019). Characterisation of the in vitro bioactive properties of alkaline and enzyme extracted brewers' spent grain protein hydrolysates. *Food Research International, 121*, 524–532. https://doi.org/10.1016/j.foodres.2018.12.008

Connolly, A., Piggott, C. O., & FitzGerald, R. J. (2013). Characterisation of protein-rich isolates and antioxidative phenolic extracts from pale and black brewers' spent grain. *International Journal of Food Science & Technology, 48*(8), 1670–1681. https://doi.org/10.1111/ijfs.12137

Cooray, S. T., & Chen, W. N. (2018). Valorization of brewer's spent grain using fungi solid-state fermentation to enhance nutritional value. *Journal of Functional Foods, 42*, 85–94. https://doi.org/10.1016/j.jff.2017.12.027

Dickinson, E. (2003). Hydrocolloids at interfaces and the influence on the properties of dispersed systems. *Food Hydrocolloids, 17*(1), 25–39. https://doi.org/10.1016/S0268-005X(01)00120-5

Dickinson, E. (2009). Hydrocolloids as emulsifiers and emulsion stabilizers. *Food Hydrocolloids, 23*(6), 1473–1482. https://doi.org/10.1016/j.foodhyd.2008.08.005

Evans, M., Ratcliffe, I., & Williams, P. A. (2013). Emulsion stabilisation using polysaccharide–protein complexes. *Current Opinion in Colloid & Interface Science, 18*(4), 272–282. https://doi.org/10.1016/j.cocis.2013.04.004

Feng, Y., & Lee, Y. (2016). Surface modification of zein colloidal particles with sodium caseinate to stabilize oil-in-water Pickering emulsion. *Food Hydrocolloids, 56*, 292–302. https://doi.org/10.1016/j.foodhyd.2015.12.030

de Folter, J. W. J., van Ruijven, M. W. M., & Velikov, K. P. (2012). Oil-in-water Pickering emulsions stabilized by colloidal particles from the water-insoluble protein zein [10.1039/C2SM07417F]. *Soft Matter, 8*(25), 6807–6815. https://doi.org/10.1039/C2SM07417F

Freitas, C., & Müller, R. H. (1998). Effect of light and temperature on zeta potential and physical stability in solid lipid nanoparticle (SLNTM) dispersions. *International Journal of Pharmaceutics, 168*(2), 221–229. https://doi.org/10.1016/S0378-5173(98)00092-1

Gould, J., Vieira, J., & Wolf, B. (2013). Cocoa particles for food emulsion stabilisation [10.1039/C3FO30181H]. *Food & Function, 4*(9), 1369–1375. https://doi.org/10.1039/C3FO30181H

Hinderink, E. B. A., Schröder, A., Sagis, L., Schroën, K., & Berton-Carabin, C. C. (2021). Physical and oxidative stability of food emulsions prepared with pea protein fractions. *LWT, 146*, Article 111424. https://doi.org/10.1016/j.lwt.2021.111424

Ibbett, R., White, R., Tucker, G., & Foster, T. (2019). Hydro-mechanical processing of brewer's spent grain as a novel route for separation of protein products with differentiated techno-functional properties. *Innovative Food Science & Emerging Technologies, 56*. https://doi.org/10.1016/j.ifset.2019.102184

Jones, D. B. (1931). *Factors for converting percentages of nitrogen in foods and feeds into percentages of proteins*. US Department of Agriculture.

Karefyllakis, D., Octaviana, H., van der Goot, A. J., & Nikiforidis, C. V. (2019). The emulsifying performance of mildly derived mixtures from sunflower seeds. *Food Hydrocolloids, 88*, 75–85. https://doi.org/10.1016/j.foodhyd.2018.09.037

Kurukji, D., Pichot, R., Spyropoulos, F., & Norton, I. T. (2013). Interfacial behaviour of sodium stearoyllactylate (SSL) as an oil-in-water Pickering emulsion stabiliser. *Journal of Colloid and Interface Science, 409*, 88–97. https://doi.org/10.1016/j.jcis.2013.07.016

Lynch, K. M., Steffen, E. J., & Arendt, E. K. (2016). Brewers' spent grain: A review with an emphasis on food and health. *Journal of the Institute of Brewing, 122*(4), 553–568. https://doi.org/10.1002/jib.363

Macias-Garbett, R., Serna-Hernández, S. O., Sosa-Hernández, J. E., & Parra-Saldívar, R. (2021). Phenolic compounds from Brewer's spent grains: Toward green recovery methods and applications in the cosmetic industry [Mini review]. *Frontiers in Sustainable Food Systems, 5*. https://doi.org/10.3389/fsufs.2021.681684

Madivala, B., Vandebril, S., Fransaer, J., & Vermant, J. (2009). Exploiting particle shape in solid stabilized emulsions [10.1039/B816680C]. *Soft Matter, 5*(8), 1717–1727. https://doi.org/10.1039/B816680C

Möller, A. C., van der Padt, A., & van der Goot, A. J. (2022). Influence of the fractionation method on the protein composition and functional properties. *Innovative Food Science & Emerging Technologies, 81*, Article 103144. https://doi.org/10.1016/j.ifset.2022.103144

Mussatto, S. I. (2014). Brewer's spent grain: A valuable feedstock for industrial applications. *Journal of the Science of Food and Agriculture, 94*(7), 1264–1275. https://doi.org/10.1002/jsfa.6486

Mussatto, S. I., Dragone, G., & Roberto, I. C. (2006). Brewers' spent grain: Generation, characteristics and potential applications. *Journal of Cereal Science, 43*(1), 1–14. https://doi.org/10.1016/j.jcs.2005.06.001

Neuberger, T., Sreenivasulu, N., Rokitta, M., Rolletschek, H., Göbel, C., Rutten, T., … Borisjuk, L. (2008). Quantitative imaging of oil storage in developing crop seeds. *Plant Biotechnology Journal, 6*(1), 31–45. https://doi.org/10.1111/j.1467-7652.2007.00294.x

Niemi, P., Martins, D., Buchert, J., & Faulds, C. B. (2013). Pre-hydrolysis with carbohydrases facilitates the release of protein from brewer's spent grain. *Bioresource Technology, 136*, 529–534. https://doi.org/10.1016/j.biortech.2013.03.076

Niemi, P., Tamminen, T., Smeds, A., Viljanen, K., Ohra-aho, T., Holopainen-Mantila, U., … Buchert, J. (2012). Characterization of lipids and Lignans in Brewer's spent grain and its enzymatically extracted fraction. *Journal of Agricultural and Food Chemistry, 60*(39), 9910–9917. https://doi.org/10.1021/jf302684x

Qi, J.-R., Song, L.-W., Zeng, W.-Q., & Liao, J.-S. (2021). Citrus fiber for the stabilization of O/W emulsion through combination of Pickering effect and fiber-based network. *Food Chemistry, 343*, Article 128523. https://doi.org/10.1016/j.foodchem.2020.128523

Schröder, A., Laguerre, M., Tenon, M., Schroën, K., & Berton-Carabin, C. C. (2021). Natural particles can armor emulsions against lipid oxidation and coalescence. *Food Chemistry, 347*, Article 129003. https://doi.org/10.1016/j.foodchem.2021.129003

Schulman, J. H., & Leja, J. (1954). Control of contact angles at the oil-water-solid interfaces. Emulsions stabilized by solid particles (BaSO4) [10.1039/TF9545000598]. *Transactions of the Faraday Society, 50*(0), 598–605. https://doi.org/10.1039/TF9545000598

Sjostrom, E. (1989). The origin of charge on cellulosic fibers. *Nordic Pulp & Paper Research Journal, 4*(2), 90–93. https://doi.org/10.3183/npprj-1989-04-02-p090-093

Sridharan, S., Meinders, M. B. J., Bitter, J. H., & Nikiforidis, C. V. (2020). Pea flour as stabilizer of oil-in-water emulsions: Protein purification unnecessary. *Food Hydrocolloids, 101*, Article 105533. https://doi.org/10.1016/j.foodhyd.2019.105533

Tan, Y. X., Mok, W. K., & Chen, W. N. (2020). Potential novel nutritional beverage using submerged fermentation with Bacillus subtilis WX-17 on brewers' spent grains. *Heliyon, 6*(6), Article e04155. https://doi.org/10.1016/j.heliyon.2020.e04155

Ullah, I., Yin, T., Xiong, S., Huang, Q., Zia ud, D., Zhang, J., & Javaid, A. B. (2018). Effects of thermal pre-treatment on physicochemical properties of nano-sized okara (soybean residue) insoluble dietary fiber prepared by wet media milling. *Journal of Food Engineering, 237*, 18–26. https://doi.org/10.1016/j.jfoodeng.2018.05.017

Vashisth, C., Whitby, C. P., Fornasiero, D., & Ralston, J. (2010). Interfacial displacement of nanoparticles by surfactant molecules in emulsions. *Journal of Colloid and Interface Science, 349*(2), 537–543. https://doi.org/10.1016/j.jcis.2010.05.089

Vieira, E., Rocha, M. A. M., Coelho, E., Pinho, O., Saraiva, J. A., Ferreira, I. M. P. L. V. O., & Coimbra, M. A. (2014). Valuation of brewer's spent grain using a fully recyclable integrated process for extraction of proteins and arabinoxylans. *Industrial Crops and Products, 52*, 136–143. https://doi.org/10.1016/j.indcrop.2013.10.012

Vignati, E., Piazza, R., & Lockhart, T. P. (2003). Pickering emulsions: Interfacial tension, colloidal layer morphology, and trapped-particle motion. *Langmuir, 19*(17), 6650–6656. https://doi.org/10.1021/la034264l

Wallecan, J., McCrae, C., Debon, S. J. J., Dong, J., & Mazoyer, J. (2015). Emulsifying and stabilizing properties of functionalized orange pulp fibers. *Food Hydrocolloids, 47*, 115–123. https://doi.org/10.1016/j.foodhyd.2015.01.009

Wang, C., Tian, Z., Chen, L., Temelli, F., Liu, H., & Wang, Y. (2010). Functionality of barley proteins extracted and fractionated by alkaline and alcohol methods. *Cereal Chemistry, 87*(6), 597–606. https://doi.org/10.1094/CCHEM-06-10-0097

Wiącek, A. E., & Chibowski, E. (2002). Zeta potential and droplet size of n-tetradecane/ethanol (protein) emulsions. *Colloids and Surfaces B: Biointerfaces, 25*(1), 55–67. https://doi.org/10.1016/S0927-7765(01)00304-6

Yang, T., Liu, T.-X., Li, X.-T., & Tang, C.-H. (2019). Novel nanoparticles from insoluble soybean polysaccharides of Okara as unique Pickering stabilizers for oil-in-water emulsions. *Food Hydrocolloids, 94*, 255–267. https://doi.org/10.1016/j.foodhyd.2019.03.035